

# Substrate-removed semiconductor disk laser with 0.6 W output power

Peng Zhang (张 鹏)<sup>1,2\*</sup>, Teli Dai (戴特力)<sup>1,2</sup>, Yu Wu (伍 瑜)<sup>1,2</sup>, Yanhai Ni (倪滨海)<sup>1,2</sup>,  
Yong Zhou (周 勇)<sup>3</sup>, Li Qin (秦 莉)<sup>4</sup>, Yiping Liang (梁一平)<sup>1,2</sup>, and Siqiang Fan (范嗣强)<sup>1,2</sup>

<sup>1</sup>College of Physics and Electronic Engineering, Chongqing Normal University, Chongqing 400047, China

<sup>2</sup>Chongqing High Education Key Laboratory of Optical Engineering, Chongqing Normal University, Chongqing 400047, China

<sup>3</sup>The 44th Research Institute of China Electronics Technology Group Corporation, Chongqing 400060, China

<sup>4</sup>Changchun Institute of Optics, Fine Mechanics and Physics, Chinese Academy of Sciences, Changchun 130022, China

\*Corresponding author: gchzh2003@yahoo.com.cn

Received August 7, 2011; accepted October 25, 2011; posted online April 18, 2012

A high power and good beam quality InGaAs/GaAs quantum well semiconductor disk laser at 1015 nm wavelength is reported. The semiconductor wafer is grown in reverse order: substrate in the window side and the distributed Bragg reflector is the last grown epilayer. Then the wafer is up-side-down and capillary bonded to a SiC heatsink, and the substrate is chemically etched. Because the total thickness of the substrate-removed structure is less than 10  $\mu\text{m}$ , the thermal management of the laser is significantly improved, and the maximum output power over 0.6 W is obtained using a 3% output coupler and 3.2 W incident pump power. The  $M^2$  factors of 1.02 and 1.01 indicate a near-diffraction-limited beam quality. To further reveal the characteristics of this substrate-etched structure on the thermal management, the heat flux and the temperature distribution of the gain wafer are numerically analyzed, and the corresponding results are discussed.

OCIS codes: 140.0140, 140.3460, 140.3480, 140.5960.

doi: 10.3788/COL201210.S11401.

For a time, solid-state disk lasers have excellent beam quality and high output power but very limited wavelengths determined by the properties of exiting doped crystals and glasses<sup>[1]</sup>. In comparison, semiconductor lasers possess various wavelengths from visible to infrared region supported by the well-developed band engineering. However, it is difficult to obtain high output power and good beam quality simultaneously for semiconductor lasers. This status has been changed since semiconductor disk lasers (SDLs) were demonstrated<sup>[2]</sup>.

Advantages of SDLs, also known as vertical external cavity surface emitting lasers (VECSELs), are evident: by the use of the optical configuration exactly like solid-state disk lasers, SDLs can produce high output power and good beam quality simultaneously<sup>[3]</sup>; by the support of the well-developed band engineering, the wavelength coverage of SDLs is from visible to infrared. In addition, the external cavity configuration of SDLs allows inserting single optical element for specific purpose, e.g., a nonlinear crystal for frequency transforming<sup>[4]</sup>, or an optical filter for wavelength tuning<sup>[5]</sup>.

GaAs-based SDLs with high power and good beam quality have been used in many interesting fields such as spectroscopy<sup>[6]</sup>, laser display<sup>[7]</sup>, laser communications<sup>[8]</sup>, and laser pump source<sup>[9]</sup>, etc. High output power is one of the most important advantages of SDLs and is the performance index always being pursued. However, just like any other kind of lasers, the output power of SDLs is limited by the thermal effects. With the deposited heat, thus increased temperature, the gain of quantum wells (QWs) will decrease sharply<sup>[10]</sup>, the laser wavelength will redshift, and the periodic resonant gain structure<sup>[11]</sup> will be detuned. What is more, the nonradiative recombination will become dominant and the temperature rise

will be further accelerated. All of the above factors are compounded until finally the thermal rollover of the laser occurs.

Two kinds of technique, substrate removal<sup>[2]</sup> and the use of heatspreader<sup>[12]</sup>, have been widely employed in the thermal management to upgrade the output power of a SDL. In the former method, the substrate (with low thermal conductivity and large thickness) of the wafer is removed by mechanical or chemical means, and the generated heat is dissipated via the heatsink. This method works very well in a 1- $\mu\text{m}$  wavelength SDL and has supported the highest output power SDL<sup>[13]</sup> so far. As to the latter method, a high thermal conductivity heatspreader is capillary bonded on the cap side of the gain chip and the generated heat is mainly dissipated via the heatspreader. Different from the former method, the latter way has been provided more suitable for long wavelength SDLs<sup>[14]</sup>.

We present a substrate-removed SDL in this letter. The semiconductor wafer was grown in reverse order (see Fig. 1): firstly the GaAs buffer layer on the GaAs substrate, then the InGaP etch-stop layer, the GaAs cap layer, the AlGaAs window layer, the InGaAs QWs active region, and finally the AlGaAs/AlGaAs distributed Bragg reflector (DBR). Then the divided gain chip is up-side-down, the DBR-side is bonded on a 350- $\mu\text{m}$  thickness SiC heatsink, and the substrate is removed by chemical etching. The SiC heatsink is soldered with a copper submount and the fabricated device is water cooled. In the experiment, the fiber coupled 808-nm laser diode pumping radiation is collimated and focused on the gain chip at 45 degree angle, and the diameter of pump spot is about 200  $\mu\text{m}$ .

For a substrate-removed SDL, the smoothness of the

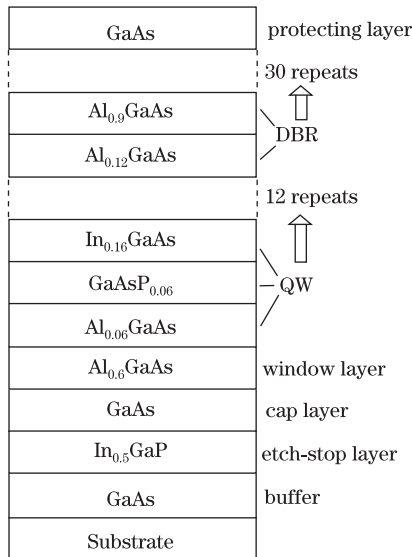


Fig. 1. Designed epitaxial structure of the semiconductor wafer.

etched surface (from where the laser emits) is crucial, because SDLs are essentially low gain lasers, so good smoothness of the etched surface (thus low scattering loss) and sufficient reflectivity of the DBR (thus low reflective loss) are elementary to support laser oscillation. In this work, slow etching is used to produce required surface quality. Figure 2 shows the top view of the substrate-etched gain chip.

Figure 3 displays the reflectivity spectra of the semiconductor wafer. The dot line is measured from the epitaxial surface (before bonded to the SiC heatsink), and the solid line is measured from the etched surface. It can be seen from the dot line that the reflectivity spectrum of the DBR is centered at 1015 nm and with a width of about 55 nm. When the substrate has been completely removed, we measure the reflectivity from the etched surface and get the solid line, which is not the exact reflectivity of the DBR, but of the DBR along with the multiple QWs, the window layer, and the cap layer. The solid line still has adequate reflectivity near 1015-nm wavelength.

The photoluminescence and laser spectra are plotted in Fig. 4. In a SDL, besides the external cavity formed by the DBR and the external mirror, there is a microcavity consisted of the DBR and the semiconductor-air interface, and the three peaks at 945, 975, and 1015 nm of the photoluminescence are corresponding to the cavity modes of the microcavity<sup>[15]</sup>. The laser mode located at 1015 nm is a coincidence of the microcavity modes and external cavity modes, and is mainly determined by the microcavity modes along with the reflectivity of the DBR. Compared with 1015 nm mode, the reflectivities of DBR at 945 and 975 nm (see Fig. 3) are too low to support the laser oscillating.

Figure 5 shows the output power versus the absorbed pump power of the SDL. A plane-concave mirror with 67 mm curvature radius and 3% transmission is used as the output coupler, and the laser cavity is approximately 65 mm. Figure 5 indicates an optical-to-optical transform efficiency of 20% and a slope efficiency of about

24%. The maximum output power of 0.64 W is achieved when the absorbed pump power is 3.2 W (which is the maximum value of the pump) and the temperature of the heatsink is 25 °C. The measured  $M^2$  factor of the output beam is depicted in Fig. 6. The values of  $M^2$  factors in the  $x$  and  $y$  directions are 1.02 and 1.01, which demonstrate a near-diffraction-limited beam quality.

As mentioned above, the output power of a SDL is essentially limited by the thermal effect. The GaAs substrate (with low thermal conductivity and big thickness) will retard the heat dissipating from the active region to the heatsink therefore accelerate the temperature rise of the laser. Figure 7 shows the simulated temperature and the heat flux of gain chip without and with 350- $\mu$ m substrate (10-W pump power and 100- $\mu$ m pump spot). As can be seen from Fig. 7(a), because of the absence of

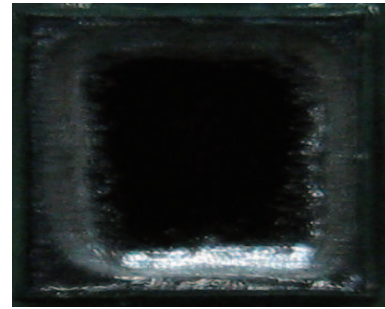


Fig. 2. Top view of the substrate-etched gain chip with 2-mm width.

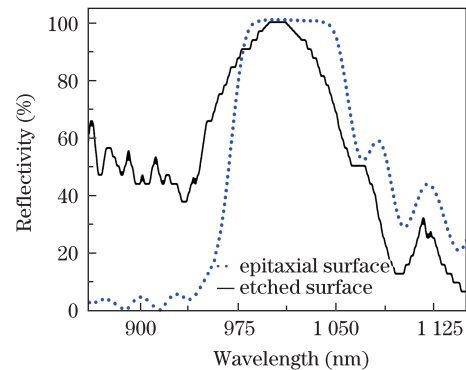


Fig. 3. Reflectivity spectra of the semiconductor wafer: epitaxial surface and etched surface.

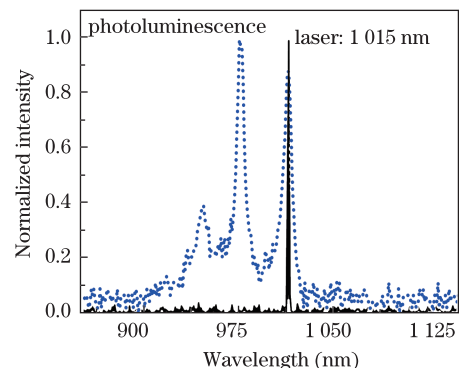


Fig. 4. Photoluminescence and laser spectra of the semiconductor wafer.

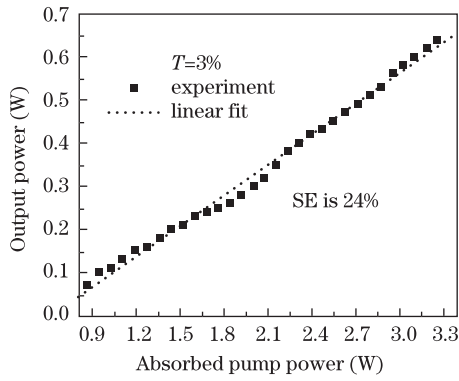


Fig. 5. Output power versus absorbed pump power of the SDL.

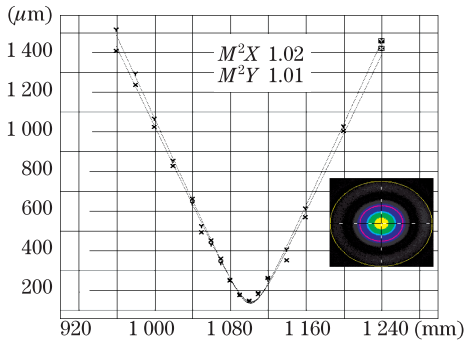


Fig. 6.  $M^2$  factor of the laser beam. The inset is the laser spot.

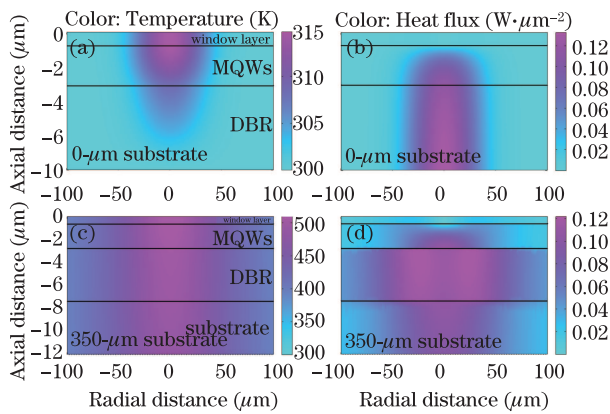


Fig. 7. Simulated temperature and heat flux of the SDL (a, b) without and (c, d) with 350- $\mu\text{m}$  substrate. The pump power and the pump spot are 10 W and 100  $\mu\text{m}$ , respectively.

the thermal resistance of substrate, the heat generated in QWs can diffuse via DBR timely; the temperature rise is concentrated in the window layer and QWs zone; and the maximum temperature rise is less than 15 K. The heat flux in Fig. 7(b) shows that almost all of the generated heats are efficiently dissipated from DBR. By comparison, Fig. 7(c) indicates that because of the existence of the thermal resistance of the thick substrate, the

maximum temperature rise is above 200 K. Figure 7(d) denotes the poor heat diffusion via DBR and substrate, i.e., the generated heat is blocked in the DBR region.

In conclusion, we demonstrate a substrate-removed SDL with 0.6-W output power. The optical-to-optical transform efficiency of 20%, the slope efficiency of 24%, and the  $M^2$  factor in  $x$  and  $y$  directions of 1.02 and 1.01 are obtained. Numerical analysis shows that this substrate removing method can significantly improve the thermal management of a SDL. Future work includes further improving the smoothness of etched surface to decrease the scatter loss (hence increase the slope efficiency), using a better bonding technology to enhance the heat exchange between the SDL and heatsink, and optimizing the output coupler to upgrade the output power.

This work was supported by the Foundation for the Creative Research Groups of High Education of Chongqing (No. 201013), the Project of Chongqing High Education Key Laboratory of Optical Engineering (No. 0705), and the PhD Foundation of Chongqing Normal University (No. 11XLB014).

## References

1. A. Giesen and J. Speiser, *IEEE J. Sel. Top. Quantum Electron.* **13**, 598 (2007).
2. M. Kuznetsov, F. Hakimi, R. Sprague, and A. Mooradian, *IEEE J. Sel. Top. Quantum Electron.* **5**, 561 (1999).
3. S. Lutgen, T. Albrecht, P. Brick, W. Reill, J. Luft, and W. Spath, *Appl. Phys. Lett.* **82**, 3620 (2003).
4. Y. Song, P. Zhang, X. Zhang, B. Yan, Y. Zhou, Y. Bi, and Z. Zhang, *Chin. Opt. Lett.* **6**, 271 (2008).
5. P. Zhang, Y. Song, X. Zhang, J. Tian, C. Jagadish, H. H. Tan, and Z. Zhang, *Opt. Eng.* **49**, 104201 (2010).
6. A. Garnache, A. A. Kachanov, F. Stoeckel, and R. Planel, *Opt. Lett.* **24**, 826 (1999).
7. U. Steegmüller, M. Kühnelt, H. Unold, T. Schwarz, R. Schulz, S. Illek, I. Pietzonka, H. Lindberg, M. Schmitt, and U. Strauss, *Proc. SPIE* **6871**, 687117 (2008).
8. J. V. Moloney, A. Peleg, P. Polynkin, L. Klein, and T. Rhoadarmer, *Proc. SPIE* **6457**, 64570N (2007).
9. D. J. M. Stothard, J. M. Hopkins, D. Burns, and M. H. Dunn, *Opt. Express* **17**, 10648 (2009).
10. P. Zhang, Y. Song, J. Tian, X. Zhang, and Z. Zhang, *J. Appl. Phys.* **105**, 053103 (2009).
11. S. W. Corzine, R. S. Geels, J. W. Scott, R. H. Yan, and L. A. Coldren, *IEEE J. Quantum Electron.* **25**, 1513 (1989).
12. P. Zhang, Y. Song, X. Zhang, J. Tian, and Z. Zhang, *Chin. Opt. Lett.* **8**, 401 (2010).
13. B. Rudin, A. Rutz, M. Hoffmann, D. J. H. C. Maas, A. R. Bellancourt, E. Gini, T. Südmeyer, and U. Keller, *Opt. Lett.* **33**, 2719 (2008).
14. A. J. Kemp, J. M. Hopkins, A. J. Maclean, N. Schulz, M. Rattunde, J. Wagner, and D. Burns, *IEEE J. Quantum Electron.* **44**, 125 (2008).
15. P. Zhang, Y. Song, X. Zhang, and Z. Zhang, *J. Opt. A: Pure Appl. Opt.* **11**, 045503 (2009).